JTTEE5 7:247-253

PEER REVIEWED

Statistical Design of Experiments for the Spheroidization of Powdered Alumina by Induction Plasma Processing

X. Fan, F. Gitzhofer, and M. Boulos

(Submitted June 1997; in revised form 9 February 1998)

The principal factors controlling the spheroidization process of Al_2O_3 powder in the induction plasma are the position of the powder injector, the powder feed rate, and their interactions. A higher level of powder feed rate (4.2 kg/h) has been achieved at the r.f. plate power of 40 kW with the application of response surface methodology (RSM). Under these loading conditions, the spheroidization of the Al_2O_3 powder of −44 + 15 μm size attained 94.9%, while for Al_2O_3 of −89 + 44 μm size, 83.3% spheroidization was achieved.

Keywords design of experiment, induction plasma process, spheroidization

1. Introduction

A thermal plasma possesses high enthalpy, which can be used to melt alumina powder (melting point 2050 °C) in a particle spheroidization process. During the induction plasma process, particles conveyed by the carrier gas are axially injected into the plasma stream. The relatively large plasma volume and high temperatures achieved during the long residence times that particles spend in the inductively coupled plasma are favorable for complete melting. Through the action of surface tension of materials in the liquid state, particles passing through and melting in the plasma generally assume the spherical or drop shape form.

There are many factors influencing the process outcome. One estimate for the number of major parameters involved in the plasma spray process is at least 35 (Ref 1), and another assessment indicated that there are ~100 interrelated processing parameters that influence the particle temperatures, velocities, and the final quality of the coatings (Ref 2). The influence of these parameters needs to be recognized and the major parameters optimized.

Statistical methods greatly increase the efficiency of experiments and often the rigor of any conclusions drawn. In recent years, the value of statistical techniques that identify the complex interplay among the thermal spray parameters and optimize those parameters have been recognized and subsequently employed by many thermal spray operators to provide the best performing coating (Ref 3-10).

Factorial design experiments (Ref 11), identifying the effects, especially the interaction effects, of the various factors on the measured response are particularly suitable for the investigation of the plasma spheroidization processes where a large number of parameters are involved. Response surface methodology (RSM) (Ref 11) is a collection of mathematical and statistical techniques useful for analyzing those problems in which several independent variables influence a dependent variable or response and is a good tool for the optimization of the plasma spheroidization process.

The first stage of the investigation distinguished the main parameters that control the spheroidization of alumina powder particles in the induction plasma process, by means of a 2^4 factorial design series of experiments. It has already been observed that it is easy to obtain 99.9% spheroidization for −44 + 15 μm alumina powder at low powder feed rates, for example, 10 g/min, along with other appropriate processing parameters. Based on these observations and analyses, RSM was used in the second stage investigations to realize a higher level of powder feed rates (4.2 kg/h) to the induction plasma process. With the employment of the optimized process parameters, as determined from RSM, the degree of spheroidization for Al_2O_3 powder of −44 + 15 μm size reached 94.9%, while 83.3% spheroidization was achieved for Al_2O_3 powder of −89 + 44 μm, even under such dense loading conditions.

2. Factorial Design of the Spheroidization Experiments

2.1 Experimental Design and Results

It has been summarized (Ref 12) that particle behavior in a plasma is mainly determined by:

- Thermodynamic properties and transport properties of the plasma
- Plasma operating parameters (velocity and temperature fields)
- Powder properties (size distribution, morphology, etc.)
- Powder feeding (location of injector, powder feed rates, and carrier gas flow rates)

X. Fan, F. Gitzhofer, and **M. Boulos,** Plasma Technology Research Center, University of Sherbrooke, Sherbrooke, Québec J1K 2R1, Canada. X. Fan is presently at Research Center of Advanced Materials, National Institute for Research in Inorganic Materials (NIRIM), Namiki 1-1, Tsukuba, Ibaraki 305, Japan. Contact e-mail: fan@nirim.go.jp.

Following consideration of the characteristics of the induction plasma process, the following four factors were selected to study their influence on the spheroidization of alumina particles:

- *Factor A:* the location of powder injector, Z_l
- *Factor B:* the pressure in the spray chamber, P
- *Factor C:* the powder feed rate, m_p
- *Factor D:* the carrier gas flow rate, Q_1

These four factors were expected to influence the particle momentum, plasma residence time, and heat exchange in the plasma. Other important factors that impact the particle melting efficiency, such as the power coupled into the plasma, the plasma gas composition and its flow rate, etc., were all fixed in value during the first series of experiments (Table 1).

The experimental apparatus consisted of the induction plasma torch installation, a hermetically sealed chamber, and the powder feeder system. Figure 1 shows the induction plasma torch, Model PL50 (TEKNA Plasma Systems Inc., Canada). The torch design is based on the use of a water-cooled ceramic plasma confinement tube, in which a 4 turn induction coil connected through a tank circuit to the radio frequency (rf) power supply (frequency 3 MHz), is incorporated. The advantage of this torch is the 80 to 85% energy coupling efficiency achieved

Table 1 Summary of the induction plasma spheroidization conditions

Condition	Value
Fixed parameters	
Plasma gas flow rates	
Plasma gas, L/min	Ar 28
Sheath gas, L/min	Ar 90 + H_2 9.6
Plate power, kW	25
Varied parameters	
Locations of powder injector, Z_l, cm	14, 17
Pressure in chamber, P, torr	200, 500
Powder feed rate, m_p, g/min	10, 30
Carrier gas flow rate, Q_1, L/min	Ar 2.3, 6.9

Table 2 Design of spheroidization experiments and results

Treatment combinations	Z_l, cm	P_l, torr	m_p, g/min	Q_1, L/min	Spheroidization, %
I	14	200	10	2.3	93.9
a	17	200	10	2.3	97.9
b	14	500	10	2.3	92.6
ab	17	500	10	2.3	92.4
c	14	200	30	2.3	95.9
ac	17	200	30	2.3	77.7
bc	14	500	30	2.3	92.1
abc	17	500	30	2.3	89.3
d	14	200	10	6.9	95.1
ad	17	200	10	6.9	99.9
bd	14	500	10	6.9	89.0
abd	17	500	10	6.9	98.5
cd	14	200	30	6.9	96.8
acd	17	200	30	6.9	81.7
bcd	14	500	30	6.9	94.1
abcd	17	500	30	6.9	86.0

Table 3 ANOVA for spheroidization experiments

Source	Effect	Sum of squares	Degree of freedom	Mean square	F
A	-3.193	122.337	1	122.337	22.967(a)
B	-0.532	3.397	1	3.397	<1
AB	2.925	102.697	1	102.697	19.280(a)
C	-5.660	384.484	1	384.484	72.181(a)
AC	-7.723	715.721	1	715.721	134.365(a)
BC	3.086	114.299	1	114.299	21.458(a)
ABC	2.844	97.043	1	97.043	18.218(a)
D	1.244	18.563	1	18.563	3.485
AD	1.155	15.997	1	15.997	3.003
BD	-0.770	7.107	1	7.107	1.334
ABD	0.131	0.207	1	0.207	<1
CD	-0.173	0.359	1	0.359	<1
ACD	-1.505	27.195	1	27.195	5.106
BCD	-0.598	4.290	1	4.290	<1
ABCD	-2.040	49.960	1	49.960	9.379(b)
Error	...	**170.454**	**32**	**5.327**	...
Total	...	**1834.109**	...	...	...

(a) Significant at 0.01. (b) Significant at 0.04

and its reliability for long-term service. A high-pressure, water-cooled stainless steel probe of inner diameter 2.5 mm and outer diameter 8 mm penetrated the torch head axially to inject the powder for processing in the plasma.

The "airtight" spray chamber is made of a "ported" double-wall, water-cooled stainless steel and is interfaced directly with the torch via the upper port. The main body of the chamber is cylindrical, with a diameter of 520 mm. The front and rear end plates are spherical caps, ensuring that the entire chamber possesses good mechanical strength under reduced pressure conditions. The minimum pressure that could be maintained by the pumping system was 10 torr (1 torr = 0.133 kPa). Exhaust gasses extracted from the chamber were first passed through a cyclone to separate the particles carried by the "off gas stream" before entering the extraction line for further scrubbing treatment and eventual atmospheric discharge.

The powder was fed to the torch by means of a CYLCO volumetric powder feeder (SYLVESTER Company, Ohio, USA). Powder feed was supplied by a "driving screw" with a pitch of 6 threads/in. with the powder reservoir operating under vibratory mode. The metered powder was transported by the carrier gas to the injector probe. A stainless steel basin containing ~2 L of distilled water was placed at the center of the chamber to receive the powder injected into and processed by the plasma plume.

Before each spheroidizing experiment, the chamber was evacuated to <30 torr, argon was introduced to the torch, and their arc was ignited. After stabilization of the plasma, Al_2O_3 powder was injected into the probe at the feed rate designated by the factorial experimental program. The mean value for the powder feed rate applied for each run was evaluated by a mass balance measurement.

The injected and plasma processed Al_2O_3 powder was collected in the water quench basin located at the chamber center. After filtering and drying, the powder was examined by optical

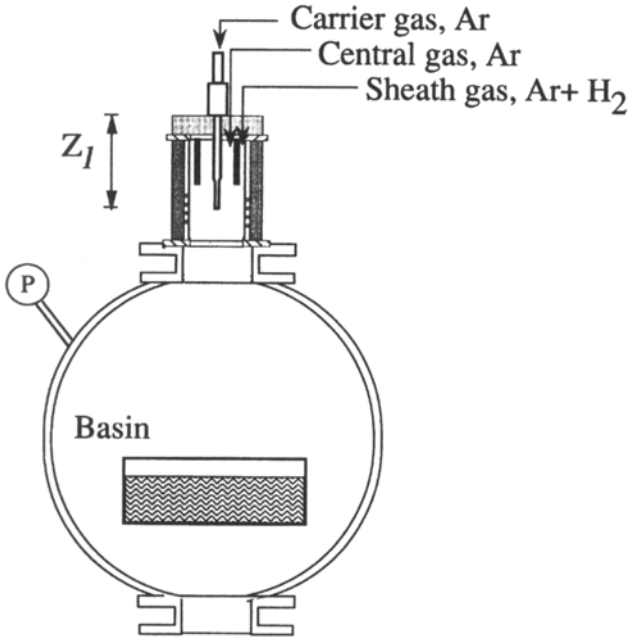

Fig. 1 Schematic drawing of spheroidization experiment set up

microscopy. Particles that had been completely melted appeared as transparent balls. By counting the number of unmelted polyhedrons and the total number of particles in a given sample, the number of spheroidized particles was derived by subtraction. Spheroidization percentage was then calculated as the ratio of the number of the spheroidized particles to the total number of particles in the field of vision. Table 2 lists three replicate measurements (~1000 processed particles counted for each measurement), performed for each spheroidized powder specimen.

Each study factor was assigned two levels, also referred to as treatments for the particle spheroidization investigation. This design provided the smallest number of experiments for a complete factorial arrangement.

The effect of a factor is denoted by a capital letter. Thus, "A" refers to the effect of factor A, "B" refers to the effect of factor B, and "AB" refers to the AB interaction, etc. In a factorial design, all possible combinations of the levels of the factors are investigated. The treatment combinations in the design are usually represented by lower case letters. Thus, "*a*" represents the treatment combination of A at the high level and others are at the lower levels. "*ab*" represents the case where both factors A and B are at the high level and others are at the lower level, etc. The analysis of variance (ANOVA) enables comparison to be made of the variance in the experimental data for each parameter with statistical probability tables. The mean squares of all the factors, their interactions, and the random error component are first calculated. The *F* statistic for testing for any main effect or interaction is found by dividing the mean square for the main effect or interactions by the mean square error. Finally, the value of the *F* statistic is compared with the tabulated "probability of significance." If the value of the *F* statistic exceeds the "probability of significance," at some confidence level, then that parameter is viewed as being significant.

Table 3 gives the ANOVA for the spheroidization percentage respectively. More intuitive graphs, plotting the responses versus the factors for this group of experiments, are given in Fig. 2, where the first half of the experimental data (Q_1 = 2.3 L/min) are illustrated. When alumina powder of –44 + 15 μm was used, the spheroidization value was 99.9%. The long residence time of the particles in the induction plasma process permits the melting of large particles in spite of the comparatively lower energy density. Figure 3 shows the morphologies of Al_2O_3 particles of larger size (–89 + 44 μm) before and after the plasma spheroidization, where the percentage of spheroidized particles attained 98%.

2.2 *Factorial Analysis for Spheroidization Experiments*

The factorial experiments allow the effects of the variations in the four parameters to be evaluated as follows.

Factor A, the location of the powder injector, Z_I. There are recirculation flows in the inductively coupled plasma torch, which aid in the dispersion of the injected particles. In order that injected powder penetrates the plasma, it is necessary to either inject it into the discharge at a sufficiently high velocity to overcome this backflow or to have the powder injector probe penetrate the discharge at the point around the middle of the induction field. In either case, this results in local cooling of the plasma at the point of injection, with a consequent slight loss of

energy efficiency (Ref 13). The position for the injection, that is, along the axis of the inductively coupled plasma torch, is an important parameter in obtaining satisfactory material treatment (Ref 14, 15).

The factorial design experiments reveal the influence of the injector position on the efficiency of spheroidization. Furthermore, it is important to note the actual interaction of this parameter with other process parameters. In certain situations, the probe position might appear to produce no distinctive effects on the responses because of the masking effect by high-order interactions. For example, the spheroidization efficiencies of the treatment combinations *b* and *ab* and *bd* and *abc* (see Table 2) are quite the same, in spite of the fact that different probe positions were used in these experiments.

Factor B, the pressure in the chamber, *P*. The effect of the interactions between the chamber pressure and other factors is significant. Chamber pressure variation is responsible for the shift in particle velocity and, thus, particle dwell time in the plasma. The most important interactions observed include chamber pressure with powder feed rate, BC, pressure with injector location, AB, and pressure with injector location and powder feed rate, ABC. These observations indicate that chamber pressure is a very important parameter in the induction plasma process, requiring careful selection and adjustment.

Factor C, the powder feed rate, m_p. The powder feed rate plays a more distinct role in the induction plasma process. The factorial experimental results indicate that this is the principal factor among the four parameters and it interferes with other parameters significantly. Previous theoretical investigation of the "dense loading condition" (Ref 16) suggested that complete melting for Al_2O_3 powder of $d_p = 60$ μm is only achieved at powder feed rates in the range of ~10 to 20 g/min or less (for a net discharge power of 5 kW). The results of the experiments described here are qualitatively in accord with this prediction. Under the same conditions, but at the high powder reed rate of 30 g/min, there are some incompletely melted particles, with some particles even remaining in the original polyhedral shape. (Compare *a* and *ac* in Table 2).

Factor D, the carrier gas flow rate, Q_1. This factor has not distinguished itself as a significant variable factor over the values employed. According to laser doppler anemometer measurements of particle velocity in the induction plasma process (Ref 17), the range of carrier gas flow rates selected in these

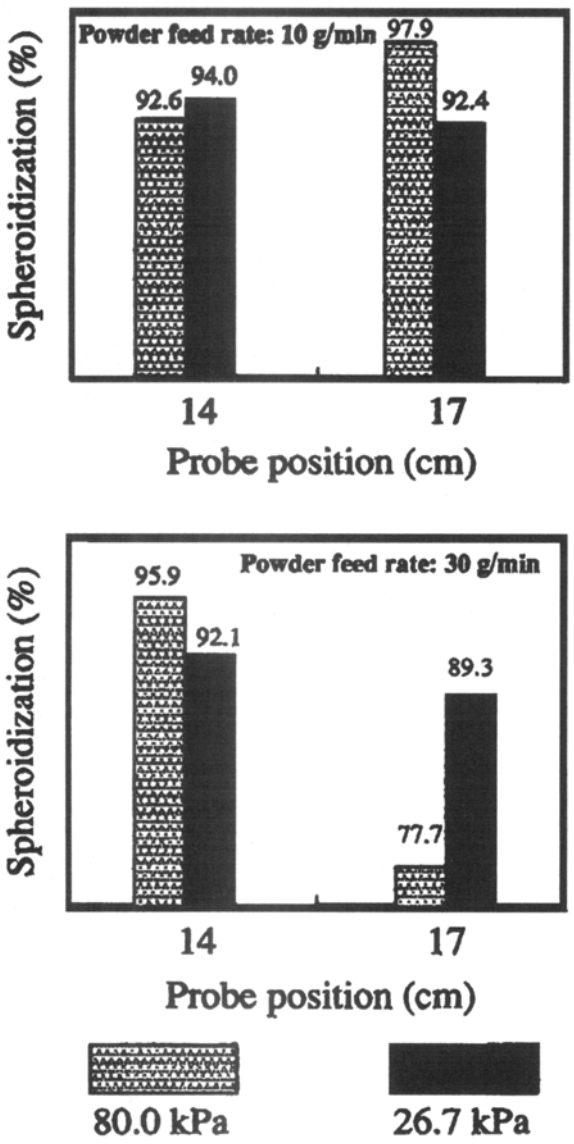

Fig. 2 Experimental result of factorial design

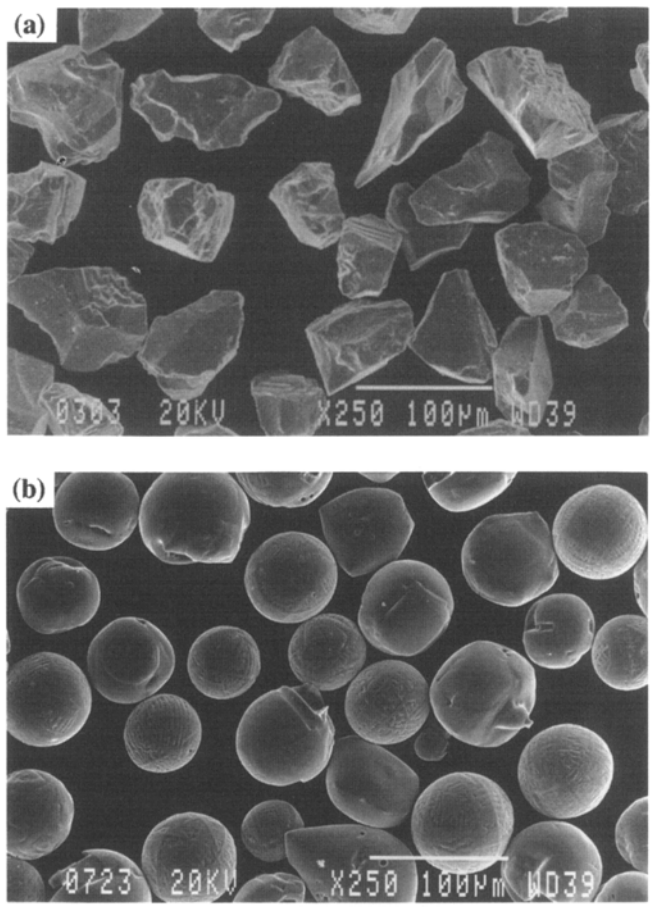

Fig. 3 Morphologies of alumina particles -89+44 μm (a) before and (b) after induction plasma spheroidization. 25 kW, 500 torr, $Z_I = 17$ cm, and $m_p = 10$ g/min

experiments should give rise to approximately two times the variation in the particle velocity (~10 m/s to 20 m/s). However, this change in particle velocity has no obvious influence on the result of particle spheroidization.

According to the statistical treatment of the experimental data in Table 3, the following conclusions can be drawn:

- Among the 4 factors considered, factor C (the powder feed rate) and factor A (the injector position) are the major parameters that significantly affect the particle spheroidization efficiency in the induction plasma process.
- The AC interaction (position of injector and powder feed rate) has a strong effect on the process. The minimum spheroidization percentage (77.7%) was found to occur under the treatment combination of *ac* (Z_I = 17 cm, m_p = 30 g/min).
- The interactions AB, position of injector and pressure in the chamber, BC, pressure in chamber and powder feed rate, and ABC are significant, although factor B, pressure in chamber, does not act in an independent manner.
- Factor D, carrier gas flow rate, has no apparent influence on the spheroidization efficiency, nor interaction with other factors. However, the highest order interaction ABCD may be significant with a confidence of 96%.

It has been observed that under the condition of higher injector position (Z_I = 14 cm), the larger feed rate favors particle spheroidization (compare *c* and *ac* or *cd* and *acd* in Table 2). This is due to (a) the high position of the probe ensures that particles are injected into the high-temperature zone of the plasma, (b) the high feed rate, so that the high momentum of the powder and carrier gas facilitates their passage through the main body of the plasma without being significantly dispersed by recirculation to the outer region of the plasma, where the temperature is much lower than that existing along the torch axis, and (c) the "loading effect" causes localized cooling of the plasma in the central region of the discharge. This results in an increase in the local gas density, with a corresponding decrease in its volumetric flow rate and the local plasma velocity, so the injected particles exhibit a longer residence time in the induction plasma (Ref 13). This phenomenon gives rise to the possibility of high powder feed rates with reasonable powder treatment cost and efficiency.

Table 4 Experimental data of RSM

Natural variables		Coded variables		Response,
Z_I, cm	P, torr	x_1	x_2	total porosity, %
12	200	−1	−1	8.8
12	200	−1	−1	9.2
12	200	−1	−1	9.9
12	500	−1	1	23.7
17	200	1	−1	18.6
17	500	1	1	24.6
14.5	350	0	0	13.2
14.5	350	0	0	13.3
14.5	350	0	0	13.3
14.5	562	0	1.414	17.2
18.1	350	1.414	0	20.7
12	350	−1	0	11.7
14.5	200	0	−1	11.0

3. Realization of Higher Powder Feed Rates

The main obstacle for using a higher powder feed rate is the powder loading effect on the plasma treatment, mentioned in the previous section; that is, the plasma-particle interaction produces cooling of the plasma. This, in turn, gives rise to a corresponding drop in the rate or degree of particle melting in the plasma. A correlation factor, Q_T/m_p, the net specific power retained by the particles per unit mass (Q_T is the total heat transfer rate to the particles and m_p is the powder feed rate), has been formulated to predict whether complete melting is possible, by combining the thermodynamic properties of the particle material (Ref 16). The specific power absorbed by the particles is inversely proportional to the powder feed rate. Because of the plasma-particle coupling effects, a decrease in the plasma temperature results in a reduction of the rate of heat transfer to the particles. The correlation factor, Q_T/m_p, at certain energy input specifies the range of feed rates beyond which complete melting of particles becomes impossible. The loading effect is much stronger for refractory/ceramic materials than for metallic powders.

On the other hand, high powder feed rates of ~4 to 6 kg/h are currently adopted by the thermal spray industry as a standard and are desired from the economic view point (Ref 18).

Response surface methodology has been used to investigate higher powder feed rates. The porosity of the deposit (sprayed onto rotating stainless steel substrate of 2.54 cm in diameter and of 0.5 cm thickness) was taken as the response, in consideration that a dense deposit can only be produced by well-melted (spheroidized) powder particles. The powder injector position Z_I and the pressure in the chamber were the variables selected for the study. This selection is based on the results from the preceding factorial design experiments on the topic of particle spheroidization, where the interaction of the injector position

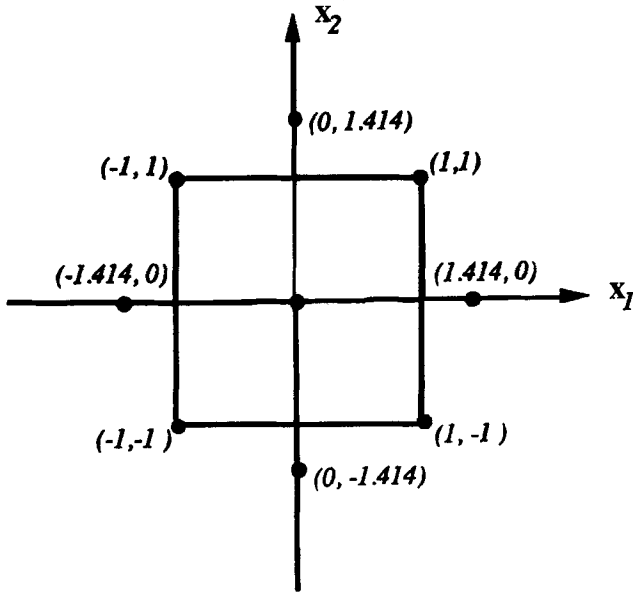

Fig. 4 Central composite design (two factors) for fitting the response surface

and the pressure in the chamber (AB) was significant in influencing the particle melting behavior. The powder feed rate was fixed at 70 g/min (4.2 kg/h). Small size Al_2O_3 powder (–44 + 15 μm) was used in the majority of these experiments. Large-sized Al_2O_3 (–89 + 44 μm) powder was used in some experiments to provide information on the influence of particle size on deposit quality under dense loading conditions. The power level of the induction plasma was fixed at 40 kW.

In accordance with the RSM, the experiments were carried out following the central composite design (Ref 11) (see Fig. 4). This design allows the fitting of a second-order model to illuminate the relation between the deposit porosity and the injector position and the pressure in the chamber. Table 4 shows the experimental design and results produced. To simplify the calculations, the coded variables have been transformed, according to the following relations:

$$x_1 = \frac{P - 350}{150}; \quad x_2 = \frac{Z_I - 14.5}{2.5} \qquad \text{(Eq 1)}$$

The region for investigation of x_1 (pressure in chamber) is {200, 560} torr and for x_2 (injector position) is {12, 18} cm. Repeated observations at the center and at other specific points

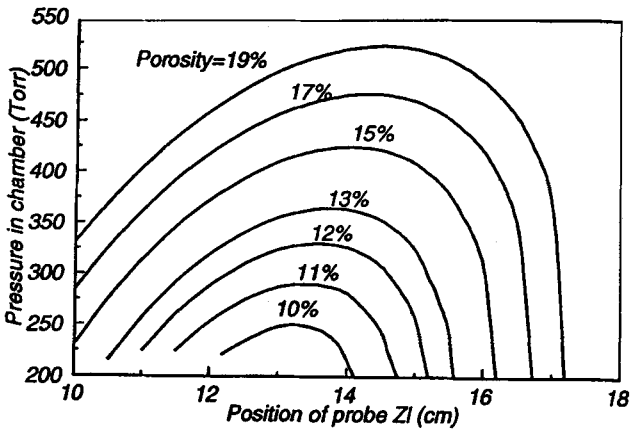

Fig. 5 The contour plot of the response surface of alumina deposit porosity. –44 + 15 μm, 40 kW, m_p = 4.2 kg/h

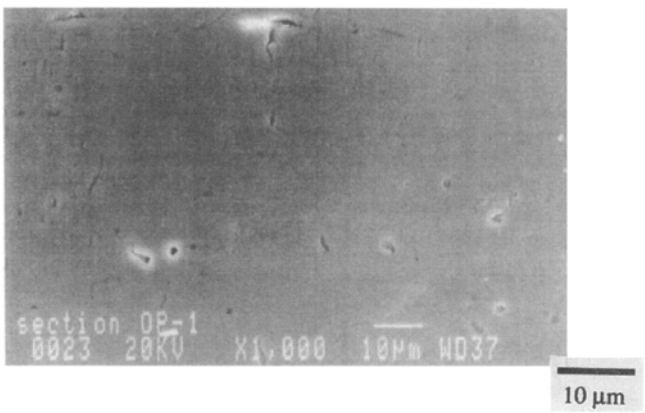

Fig. 6 The cross section of the corresponding alumina deposit at the powder feed rate of m_p = 4.2 kg/h. –44 + 15 μm, 40 kW, 200 torr, Z_I = 12 cm. (Art has been reduced to 74% of its original size for printing.)

were used to estimate the experimental error and to allow the second-order model to be checked.

According to the principle of the central composite design (Fig. 4), the last two experiments should have been carried out at the points [0, –1.414] and [–1.414, 0]; that is, [10.9 cm, 350 torr] and [14 cm, 187.9 torr], respectively. However, these points are outside the reasonable range of the induction plasma process. They have been replaced by the points [–1, 0] and [0, –1]. A second-order model is fitted to the coded data by least square regression method, yielding:

$$\text{Porosity } (\%) = 12.80 + 2.23x_1 + 3.62x_2 + 3.40x_1^2 + 1.36x_2^2 - 1.96x_1x_2 \qquad \text{(Eq 2)}$$

Figure 5 shows the plotted contours of the response surface. This is a "falling ridge system" where the stationary point (the optimum point on the response surface, if it exists) is outside the region of exploration. However, further attempts to shift the experiment points towards the low porosity response were thwarted by the physical limitation of the process.

This group of experiments indicated that higher levels of powder feeding to the induction plasma process are possible. The best result was obtained at the Z_I = 12 cm and P = 200 torr, where the average porosity of the Al_2O_3 deposit was 9.3% (σ = 0.5%). Figure 6 shows the cross section of the corresponding deposits. The spheroidization is 94.9% for Al_2O_3 powder of –44 + 15 μm and 83.3% for powder of –89 + 44 μm at the powder feed rate of 4.2 kg/h.

Due to the complexity of the flow pattern in the discharge region of an induction plasma torch, it is always necessary to adjust parameters so that the powder particles easily penetrate the hot zone and do not bounce off the recirculation zone. The region explored for this work covered most of the possible domain for the two parameters: injector position and pressure in the chamber. The selection criteria for Z_I and the pressure in the chamber at the high powder feed rates may be summarized as:

- With a higher level of powder feeding, the optimized Z_I in this study could be located within the range of ~12 to 14 cm. This is the position where the injector tip is just a little above or below the first turn of the induction coil. Therefore, in the induction plasma process, the powder particles should be fed at a position as close as possible to the zone of highest plasma temperature, so that the injected particles receive the full temperature effect of the plasma.

- Low chamber pressures are needed to prevent the rebound behavior of particles injected into the plasma. The low-pressure allows the particles to retain a sufficient initial momentum to penetrate the high-temperature zone of the inductive plasma and to have essentially axial trajectories close to the center line of the torch, subsequently impacting on the substrate and forming a dense deposit. The low limit for the chamber pressure appears to be 200 torr. Any further decrease in pressures made the induction plasma very difficult to sustain, especially with the dense loading of particles.

4. Conclusions

Statistical methods are very useful tools in the investigation of multi-factor systems, such as the plasma process, where the interaction effect between the relevant parameters is considerable.

The powder feed rate and the injector position are the determining factors for the spheroidization of alumina particles in the induction plasma process. The interactions among the factors, particularly that of the chamber pressure with other parameters, are significant. It is easy to obtain 99.9% spheroidization for –44 + 15 μm alumina powder at a low powder feed rate (10 g/min), together with other proper processing parameters.

Higher powder feed rates in the induction plasma process are possible. With a rate of 4.2 kg/h, at a plasma plate power of 40 kW, the degree of spheroidization for Al_2O_3 powder of –44 + μm size was 94.9%, while for Al_2O_3 powder of –89 + 44 μm, 83.3% was achieved. The high injector position and low chamber pressures are the key points to assure the penetration of powder particles into the high-temperature zone of the induction plasma.

Acknowledgment

The authors thank their colleague Dr. Peter Lanigan for his proofreading and commentary of this article. The financial support by FCAR and NSERC is gratefully acknowledged.

References

1. A. Vardelle, M. Vardelle, and P. Fauchais, Influence of Velocity and Surface Temperature of Alumina Particles on the Properties of Plasma Sprayed Coatings, *Plasma Chem. Plasma Process,* Vol 2 (No. 3), 1982, p 255
2. H. Herman, Plasma Spray Deposition Processes, *MRS Bull.,* December 1988, p 60-67
3. Anonymous, Forecast: Processes, *Adv. Mater. Process.,* Vol 1, 1991, p 59-68
4. R. Kingswell, K.T. Scott, and L.L. Wassell, Optimizing the Vacuum Plasma Spray Deposition of Metal, Ceramic, and Cermet Coatings Using Designed Experiments, *Thermal Spray: International Advances in Coatings Technology,* C.C. Berndt, Ed., ASM International, 1992, p 421-426
5. T.C. Nerz, J.E. Nerz, B.A. Kushner, A.J. Rotolico, and W.L. Riggs, Evaluation of HEP Sprayed Tungsten Carbide/Cobalt Coating Using Design of Experiment Method, *Thermal Spray: International Advances in Coatings Technology,* C.C. Berndt, Ed., ASM International, 1992, p 405-413
6. T.J. Steeper, D.J. Varacalle, Jr., G.C. Wilson, W.L. Riggs, A.J. Rotolico, and J.E. Nerz, A Design of Experiment Study of Plasma Sprayed Alumina-Titania Coatings, *Thermal Spray: International Advances in Coatings Technology,* C.C. Berndt, Ed., ASM International, 1992, p 415-420
7. K.J. Hollis, A. Bartlett, R.G. Castro, and R.A. Neiser, Investigation of the Silicon Loss in APS $MoSi_2$ under Typical Spray Conditions, *Thermal Spray: Practical Solutions for Engineering Problems,* C.C. Berndt, Ed., ASM International, 1996, p 429-437
8. D.J. Varacalle, Jr., E. Acosta, J. Figert, M. Syma, J. Worthington, and D. Carrillo, Experimental/Analytical Investigations of Air Plasma Spray Tungsten Carbide-Cobalt Coatings at Kelly Air Force Base, *Thermal Spray: Practical Solutions for Engineering Problems,* C.C. Berndt, Ed., ASM International, 1996, p 699-707
9. D.J. Varacalle, Jr. and K. Barnett, A Complete Predictor Methodology for The Plasma Spray Process, *Thermal Spray: Practical Solutions for Engineering Problems,* C.C. Berndt, Ed., ASM International, 1996, p 709-715
10. D.J. Varacalle, Jr., D.L. Hagrman, J.R. Fincke, W.D. Swank, V. Zanchuck, and E. Sampson, An Experimental Study of Twin-Wire Electric Arc Sprayed Zinc and Aluminum Coatings, *Thermal Spray: Practical Solutions for Engineering Problems,* C.C. Berndt, Ed., ASM International, 1996, p 717-723
11. D.C. Montgomery, *Design and Analysis of Experiment,* John Wiley & Sons, 1984
12. F. Gitzhofer, "Contribution à l'Étude de la Formation des Dépots Plasma de Zircone Stabilisée Utilsés dans les Barrières Thermiques," Ph.D. thesis NO. 88-11, University of Limoges, 1988 (in French)
13. M.I. Boulos, Thermal Plasma Processing, *IEEE Tran. Plasma Science.,* Vol 19 (No. 6), 1991, p 1078-1088
14. A.N. Babaevesky, P.A. Vityaz, and O.V. Romasn, Peculiarities of Spraying Coatings with a Radio-Frequency Induction Plasmatron, *Proceedings of the 10th Thermal Spraying Conference* (Essen, West Germany), 1983, p 85-87
15. S. Takeuchi, T. Okada, T. Yoshida, and K. Akashi, Development of a Novel Spray Coating Technique with a Radio-Frequency Plasma Torch, *J. Japan Inst. Met.,* Vol 52 (No. 7), 1988, p 711-718
16. P. Proulx, J. Mostaghimi, and M.I. Boulos, Heating of Powder in an r.f. Inductively Coupled Plasma under Dense Loading Conditions, *Plasma Chem. Plasma Process.,* Vol 7 (No. 1), 1987, p 29-52
17. J. Lensinski and M.I. Boulos, Laser Doppler Anemometer under Plasma Conditions. Part II. Measurements in an Inductively Coupled r.f. Plasma, *Plasma Chem. Plasma Process,* Vol 8 (No. 2), 1988, p 133-144
18. P. Fauchais, A. Grimaud, A. Vardelle, and M. Vardelle, La Projection par Plasma: Une Revue, *Ann. Phys. Fr.,* Vol 14, 1989, p 261-310 (in French)